

 Open access • Posted Content • DOI:10.1101/492751

Real-time capture of horizontal gene transfers from gut microbiota by engineered CRISPR-Cas acquisition — Source link

Christian Munck, Ravi U. Sheth, Daniel E. Freedberg, Harris H. Wang

Institutions: Columbia University

Published on: 10 Dec 2018 - bioRxiv (Cold Spring Harbor Laboratory)

Topics: Horizontal gene transfer and CRISPR

Related papers:

- [Studying plasmid horizontal transfer in situ : a critical review](#)
- [Protocols for Visualizing Horizontal Gene Transfer in Gram-Negative Bacteria Through Natural Competence](#)
- [Directed evolution of biocircuits using conjugative plasmids and CRISPR-Cas9: design and in silico experiments](#)
- [Genome-wide CRISPR-Cas9 screen in E. coli identifies design rules for efficient targeting](#)
- [CRISPR/Cas9 Targeted Capture Of Mammalian Genomic Regions For Characterization By NGS](#)

Share this paper:    

View more about this paper here: <https://typeset.io/papers/real-time-capture-of-horizontal-gene-transfers-from-gut-3hc0j8gysj>

1 **Real-time capture of horizontal gene transfers from gut microbiota by** 2 **engineered CRISPR-Cas acquisition**

3

4 Christian Munck^{1,#}, Ravi U. Sheth^{1,2,#}, Daniel E. Freedberg³, Harris H. Wang^{1,4,*}

5

6 ¹Department of Systems Biology, Columbia University, New York, NY, USA.

7 ²Integrated Program in Cellular, Molecular, and Biomedical Studies, Columbia University, New
8 York, NY, USA.

9 ³Department of Medicine, Columbia University, New York, NY, USA

10 ⁴Department of Pathology and Cell Biology, Columbia University, New York, NY, USA

11 *Correspondence to: hw2429@columbia.edu

12 #These authors contributed equally

13

14 **Abstract**

15 Horizontal gene transfer (HGT) is central to the adaptation and evolution of bacteria. However,
16 our knowledge about the flow of genetic material within complex microbiomes is lacking; most
17 studies of HGT rely on bioinformatic analyses of genetic elements maintained on evolutionary
18 timescales or experimental measurements of phenotypically trackable markers (e.g. antibiotic
19 resistance). Consequently, our knowledge of the capacity and dynamics of HGT in complex
20 communities is limited. Here, we utilize the CRISPR-Cas spacer acquisition process to detect
21 HGT events from complex microbiota in real-time and at nucleotide resolution. In this system, a
22 recording strain is exposed to a microbial sample, spacers are acquired from foreign transferred
23 elements and permanently stored in genomic CRISPR arrays. Subsequently, sequencing and
24 analysis of these spacers enables identification of the transferred elements. This approach
25 allowed us to quantify transfer frequencies of individual mobile elements without the need for
26 phenotypic markers or post-transfer replication. We show that HGT in human clinical fecal
27 samples can be extensive and rapid, often involving multiple different plasmid types, with the
28 IncX type being the most actively transferred. Importantly, the vast majority of transferred
29 elements did not carry readily selectable phenotypic markers, highlighting the utility of our
30 approach to reveal previously hidden real-time dynamics of mobile gene pools within complex
31 microbiomes.

32 Introduction

33 Densely populated polymicrobial communities exist ubiquitously in natural environments
34 ranging from soil to the mammalian gastrointestinal tract. Bacteria in these microbiomes are
35 thought to engage in extensive horizontal gene transfer (HGT) based on metagenomic
36 sequencing studies and comparative genomics analyses¹⁻⁴. HGT is a natural phenomenon
37 where DNA is exchanged between organisms through distinct mechanisms including cell-to-cell
38 conjugation of mobile plasmids or genetic elements, transduction by phages and viruses, or
39 transformation by uptake of extracellular nucleic acids⁵. Upon horizontal transfer, the foreign
40 genetic element can be either retained in the recipient or lost over time. HGT processes play a
41 driving role in the evolution of bacterial genomes, leading to the dissemination of important
42 functions such as complex carbohydrate metabolism⁶, pathogenicity⁷, and resistance to
43 antibiotics⁸ or toxic compounds⁹.

44 Despite the prevalence of HGT, the evolutionary selection that drives fixation of foreign
45 DNA is generally not well understood; for example, roughly 30% of genes predicted to be
46 acquired by HGT have no known function³, and pan-genome analysis of sequenced genomes
47 predict that many species have open-ended pan-genomes with enormous potential for gene
48 turnover¹⁰⁻¹². For fixation of transferred DNA in recipient cells to ultimately occur, many barriers
49 must be overcome, such as specific selection pressures, fitness burden of the acquired
50 element, genetic compatibility with host machinery (e.g. replication, transcription, translation)
51 and presence of anti-HGT systems such as restriction modification systems or CRISPR-Cas
52 systems⁵. In addition, the presence of addiction elements on the transferred DNA (e.g. toxin-
53 antitoxin and partitioning systems) also influence the fate of the transferred element. Even when
54 the transferred genetic element provides a fitness benefit they may require many generations to
55 be fixed in a population¹³. The architecture and dynamics of these gene flow networks are often
56 not known, especially since most HGT genes are identified from endpoint analyses.

57 Contemporary computational methods for inference of HGT events rely on identification
58 of shared mobile elements such as plasmids or phages, analysis of genomic abnormalities (e.g.
59 shifts in GC% or codon usage) or phylogenetic comparisons between a candidate gene and a
60 conserved gene (e.g. 16S rRNA)¹⁴. On the other hand, experimental approaches to study HGT
61 require the transferred DNA to confer a detectable phenotype that can be enriched in the
62 population. However, not all mobile elements confer a readily selectable phenotype. New
63 selection-independent methods that can capture real-time transfer dynamics across a
64 population will provide a deeper and richer understanding of the overall HGT process.

65 As a consequence of the pervasive gene flow in microbial genomes, bacteria have
66 evolved various defense systems to manage horizontally acquired genetic material^{5,15}. CRISPR-
67 Cas systems can provide specific and adaptive immunity to invading DNA¹⁵. During the
68 conserved CRISPR adaptation process, Cas1 and Cas2 proteins capture short fragments of the
69 invading DNA and integrate them as spacers into CRISPR arrays. Immunity is conferred by
70 transcribed spacers in conjunction with the Cas interference machinery¹⁶. Importantly, these
71 CRISPR arrays provide a useful long-term record of horizontally acquired DNA. Most natural *E.*
72 *coli* strains do not actively acquire new spacers and their arrays therefore reflect ancient HGT
73 events¹⁷. However, overexpression of the Cas1 and Cas2 proteins can activate spacer
74 acquisition in *E. coli*¹⁸.

75 Here, we leverage the CRISPR spacer acquisition process as a mechanism for real-time
76 recording of HGT events at nucleotide-resolution. Using an optimized acquisition system, we
77 can capture transient HGT events and identify DNA transfers that cannot be easily detected with
78 traditional methods. The performance and technical accuracy of this system was rigorously
79 characterized using defined strains and communities. Application of the system to clinical
80 human fecal samples revealed prevalent and diverse HGT events, shedding light on the
81 dynamics and frequency of HGT in the mammalian gut microbiome.

82

83 **Results**

84 **Exogenous HGT DNA can be identified using CRISPR spacer acquisition**

85 We previously engineered a CRISPR-based temporal recording system that acquired
86 new spacers from either endogenous genomic DNA or a copy-number inducible plasmid¹⁹. In
87 this system, we utilized a “recording strain” (hereafter referred to as EcRec) consisting of the *E.*
88 *coli* BL21 strain with the pRec- Δ *lacI* plasmid, which contains an anhydrotetracycline (aTc)
89 inducible operon of the *E. coli* Type I-E *cas1* and *cas2* genes. Upon induction of the recording
90 strain, over-expressed Cas1 and Cas2 proteins incorporate DNA protospacer sequences into a
91 CRISPR array on the genome at high frequencies. Since *E. coli* BL21 lacks interference
92 machinery, acquired spacers do not lead to CRISPR-mediated adaptive immunity²⁰. The system
93 can thus serve as a recorder of intracellular DNA. CRISPR expansions can be easily analyzed
94 by PCR amplification of the CRISPR array from a population of recording cells, and, if needed,
95 enrichment for arrays with new spacers can be achieved by a simple gel extraction of expanded
96 array products. Subsequent deep amplicon sequencing can be used to assess the spacer
97 repertoire¹⁹. While spacers can be acquired from both endogenous and exogenous DNA
98 sources, including the genome, there is a strong preference to acquire spacers from high copy

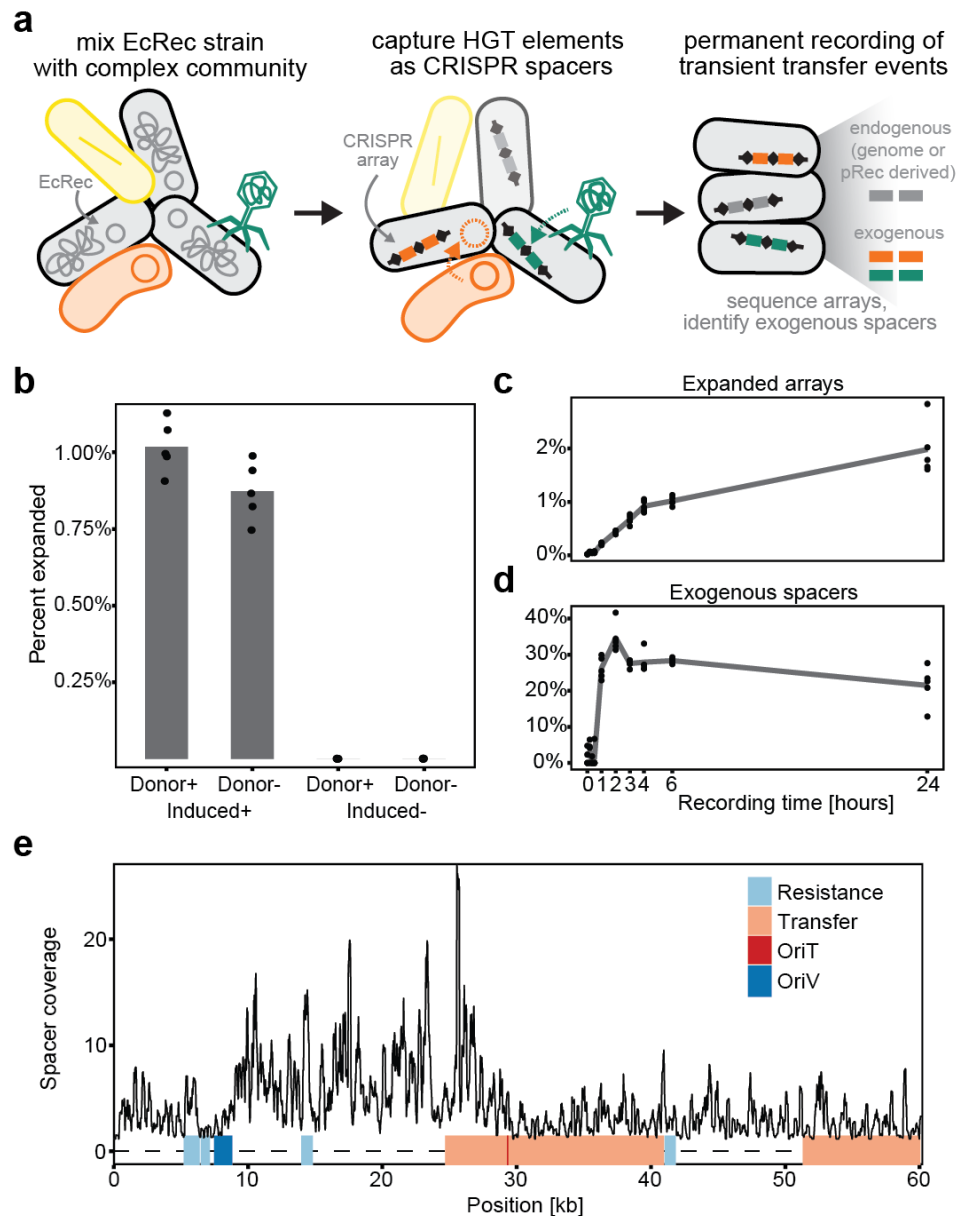
99 replicative plasmids and invading phages²¹. Given the capacity of the enhanced spacer
100 acquisition system to record intracellular DNA at much higher efficiency than the wild-type
101 system, we hypothesized that the system could be used as a sensitive method to reveal HGT
102 events (**Fig. 1a**) that may only occur transiently or at a low-frequency across a cell population.

103 To explore whether CRISPR recording can allow direct measurement of HGT events, we
104 exposed the recording strain (EcRec) to another strain (*E. coli* FS1290) that harbors the well-
105 characterized broad host range conjugative plasmid RP4²². This conjugation was carried out by
106 mixing the strains in a 1:1 ratio and spotting them on agar plates with and without induction of
107 Cas1/Cas2. Reactions without the donor *E. coli* FS1290 strain served as an additional control.
108 After 6 hours of conjugation, cells were collected and CRISPR arrays were amplified and
109 sequenced (without gel extraction) to evaluate the spacer repertoire, yielding 10⁴-10⁵ sequenced
110 arrays per biological replicate (**Suppl. Table 1**). In the Cas1/Cas2 induced cells with donor,
111 1.0% (sd = 0.1%, n = 5 recordings) of the arrays were expanded in contrast to only 0.0010% (sd
112 = 0.0006%, n = 5 recordings) in the non-induced cells (**Fig. 1b**). Further probing the dynamics of
113 the HGT recording process showed that overall spacer expansion could be identified as early as
114 1 hour after mixing the donor and recording cells, with the rate of array expansion leveling off
115 after 4 to 6 hours of bacterial conjugation (**Fig. 1c**). By 24 hours, 1.9% of all arrays (sd = 0.5%,
116 n = 5 recordings) were expanded (**Suppl. Table 1**).

117 As expected, most spacers were derived from the EcRec genome and pRec plasmid.
118 We therefore applied a stringent two-step filter against a *de novo* sequenced EcRec/pRec
119 reference to isolate putative exogenous spacer sequences. First, only spacers flanked by the
120 canonical direct repeat sequences were kept. Second, spacers with even moderate sequence
121 homology ($\geq 80\%$ identity and coverage) to the EcRec genome or the pRec plasmid were
122 removed (Materials and Methods and **Suppl. Fig S1**). Using these filtering criteria, we found
123 that among the expanded arrays, exogenous spacers constituted up to 30-40% of all new
124 spacers and could be detected within 1 hour of conjugation (**Fig. 1d**). After 24 hours, 21% (sd =
125 5%, n = 5 recordings) of the sequenced spacers were identified as exogenous. The amount of
126 exogenous spacers is influenced by the ratio of donor to recording cells, and we could detect
127 new exogenous spacers in as few as 1 donor per 10⁶ recording cells (**Suppl. Fig S2**). In
128 comparison, only 0.5 % (sd = 0.2%, n = 5 recordings) of the spacers in the induced no-donor
129 experiment were identified as exogenous, likely representing spacer sequences containing
130 technical sequencing errors (**Suppl. Table 1**).

131 In complex microbiomes, the identity of potential transferred elements is unknown.
132 However, acquired exogenous spacers can be matched against large sequence databases (e.g.

133 GenBank) to identify specific mobile elements. To define the criteria for a match between a
134 spacer and a reference database, we first gel extracted and sequenced spacers from the 24
135 hour *E. coli* FS1290 recording sample (**Suppl. Table 2**). A set of scrambled spacers was
136 generated by randomly reordering the sequence of exogenous spacers. Using BLAST, both
137 original and scrambled spacers were searched against the Genbank RefSeq bacterial genomes
138 database. We identified a conservative threshold of $\geq 95\%$ identity and coverage that prevented
139 spurious matches of scrambled spacers to the database (**Suppl. Fig. S3**). Using this threshold,
140 we found that 98.6% (sd = 0.2%, n = 5) of the unique exogenous spacers could be mapped
141 back to the RP4 plasmid sequence (**Fig. 1e**) and that spacers were acquired across the
142 plasmid, preferably from sites corresponding to the known PAM recognition sequence of *E. coli*
143 Cas1/Cas2 (AAG, 50% of all spacers, **Suppl. Fig. S4**). Together, these results show that the
144 EcRec is capable of recording horizontal gene transfer events robustly with high sensitivity and
145 that exogenous spacers can be confidently mapped to the mobile DNA of origin.
146



147

148 **Figure 1. Recording HGT with engineered CRISPR acquisition.** (a) Schematic of HGT recording
 149 where the EcRec strain is mixed with donor cells and spacers are acquired from both endogenous and
 150 exogenous DNA sources. Resulting CRISPR arrays are sequenced to determine the identity and origin of
 151 spacers. (b) Results from recording for 6 hours with or without induction and with or without FS1290/RP4
 152 as donor strain (n = 5, with mean bar, no gel-extraction). (c) Array expansion is detected within 1 h after
 153 induction and increases rapidly for the first 4-6 hours (n = 5, with mean line, no gel-extraction). (d) Unique
 154 exogenous spacers are detected 1 h after induction, constituting ~30% of all spacers. (e) Mapping of
 155 recorded unique spacers to the RP4 plasmid. Spacer coverage is average coverage per bp. in 200 bp.
 156 windows and based on 5 replicates. On average, 99% of the unique exogenous spacers map to the RP4
 157 and cover the whole plasmid backbone.

158

159 Detection of non-replicative and complex HGT events

160

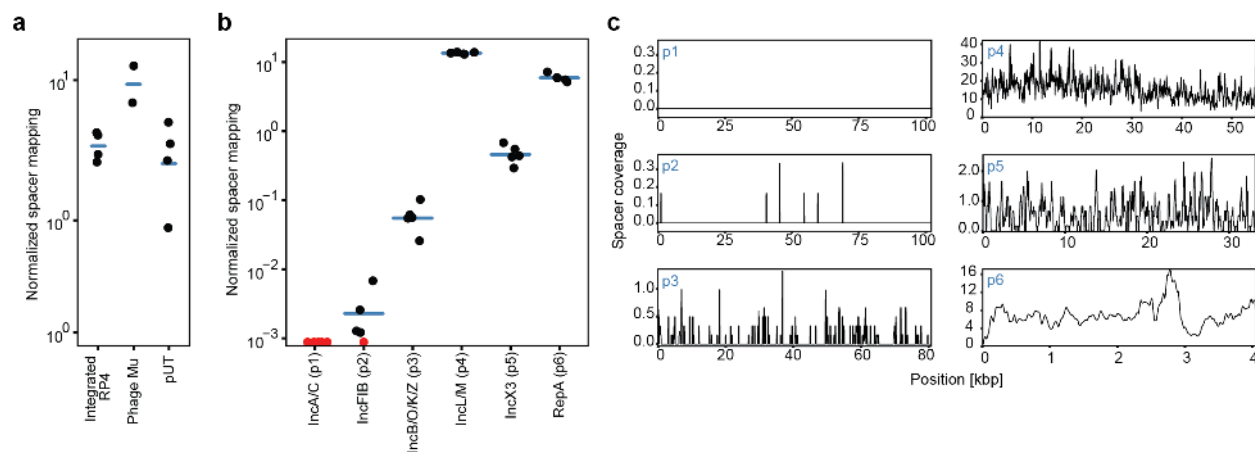
Many HGT events may be transient and may occur at low frequencies. We hypothesized
 161 that our recording system could capture spacers from HGT events in which the transferred

162 element is not stably maintained in a recipient. To investigate transfer of both genomic DNA and
163 a non-replicative plasmid we used an *E. coli* S17 strain carrying the R6K-derived plasmid pUT,
164 as the donor²³. *E. coli* S17 contains a genomically integrated copy of the RP4-Tet::Mu
165 conjugation system and also expresses the R6K replication initiation protein Pir. The integrated
166 RP4 can mobilize the S17 genome and the pUT plasmid into recipient cells²⁴. However, pUT
167 requires the Pir protein *in trans* in order to replicate and therefore cannot be maintained in the
168 EcRec recipient, which lacks the *pir* gene^{23,25}. In addition, phage Mu, which is also present in
169 S17, can be acquired by recipients either via conjugation of the S17 genome or via phage
170 particles²⁵.

171 We mixed EcRec with the *E. coli* S17/pUT donor strain and recorded spacers for 6
172 hours. Analysis of new exogenous spacers from the S17/pUT donor showed acquisition from
173 both the integrated RP4-Tet::Mu and the pUT plasmid, highlighting that active replication of the
174 transferred element is not required for spacer acquisition (**Fig. 2a**).

175 Since natural bacterial isolates often carry multiple plasmids capable of horizontal
176 transfer, we tested if our HGT recording system could resolve transfer of different mobile
177 elements from the same donor. A clinical *E. coli* isolate (Ec70) that carried 6 different plasmids
178 (p1-p6), as resolved by hybrid assembly (Oxford Nanopore and Illumina sequencing, Materials
179 and Methods), was used as the donor strain. Sequencing and analysis of new spacers from a
180 recording experiment with Ec70 revealed that 97% of exogenous spacers were acquired from
181 only two plasmids, the 55 kb plasmid p4 and the 4 kb plasmid p6. We quantified the spacer
182 mapping to the reference sequence as the average number of spacers per kb per 1,000
183 sequenced exogenous spacers, hereafter referred to as “normalized spacer mapping” (**Fig. 2b**).
184 For p4 and p6 the normalized spacer mapping was 13.5, sd = 0.4, and 6.0, sd = 0.8,
185 respectively (n = 5). While plasmid p4 is self-transmissible, the much smaller plasmid p6 only
186 carries the mobilization protein MobA, hence requiring the conjugation apparatus *in trans*.
187 Neither of the two plasmids carry any antibiotic resistance genes, which importantly highlights
188 that our recording system can readily detect elements that would not be easily detectable by
189 standard selection-based methodologies. Plasmids p3 and p5 (80 kb and 33 kb, respectively)
190 appeared to transfer, although at very low frequencies with a normalized spacer mapping of
191 0.060 and 0.48, respectively (sd = 0.03 and 0.15, n = 5 recordings). No spacers were observed
192 from the large 106 kb plasmid p1 and only eight spacers were observed from the 102 kb
193 plasmid p2 (**Fig. 2b**) from a total of ~1 million expanded spacers. As expected, spacers were
194 acquired from across the plasmid backbones (**Fig. 2c**). Together, these results demonstrate that

195 CRISPR-based recording of HGT can quantitatively reveal the relative transfer efficiencies of
196 different mobile elements from a donor that carries 6 plasmids.
197



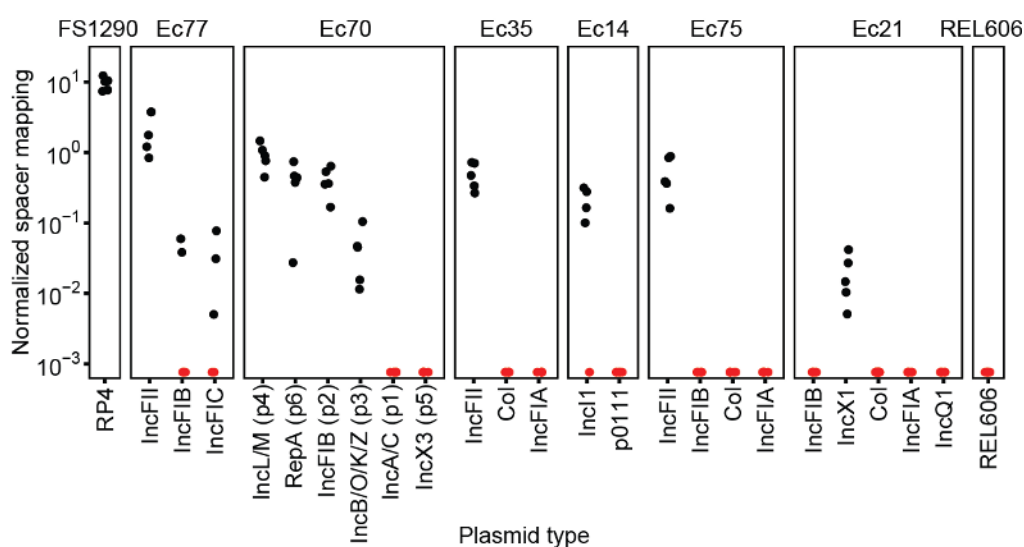
198
199 **Figure 2. Detecting non-replicative and complex HGT events.** (a) EcRec acquires spacers from
200 transferrable but non-replicating DNA elements in *E. coli* S17, the integrated RP4, phage Mu and the non-
201 replicating plasmids pUT. In total 77,825 spacers were obtained. The normalized spacer mapping is
202 spacers per kb per 1000 exogenous spacers. (n = 4 with mean bar, recorded for 6 h). (b) Recorded
203 spacers from Ec70 carrying six plasmids (p1-p6). For each plasmid the number of matching spacers is
204 normalized as spacers per kb per 1000 exogenous spacers. Red data points denote zero recorded
205 spacers. No spacers are recorded from plasmid p1 (n = 5, with mean bar, recorded for 6 h). (c) Mapping
206 of recorded spacers to the plasmid sequences, substantial coverage is seen for all plasmids except the
207 large plasmids p1 and p2 (spacer coverage is average coverage per bp. in 200 bp. windows, based on 5
208 replicates.).

209 Capturing HGT events from a defined microbial community

210
211 Having characterized the recording system using a single donor, we explored whether
212 HGT events could be recorded in a complex, multi-donor community. A defined bacterial
213 community comprised of 6 clinical *E. coli* isolates (Ec77, Ec70, Ec35, Ec14, Ec75, Ec21) as well
214 as a positive control strain (FS1290) that carries the RP4 plasmid, and a negative control strain
215 (REL606) that contains no plasmids was assembled. We generated draft genome assemblies
216 and predicted that the clinical *E. coli* strains carried at least two plasmids each, including Ec70
217 already established to contain six plasmids²⁶ (Fig. 3).

218 Donor strains were pooled in equal ratios and then mixed with EcRec. Recording was
219 carried out for 6 hours on LB agar and new exogenous spacers were identified and mapped
220 back to the contigs from the draft genome assemblies for each of the 7 donor strains while the
221 hybrid assembly was used for Ec70 strain. Spacers mapping to more than one contig were
222 filtered out to ensure an unambiguous interpretation of HGT events (26.0%, n = 3205). We
223 detected new spacers from all donor strains except from the negative control REL606 (Fig. 3).
224 However, spacers were not acquired equally from the donors, with 72% (sd = 9%, n = 5

225 recordings) of all spacers deriving from the FS1290 positive control strain, confirming that RP4
 226 transfers at high frequency²⁷. Clinical strains Ec77 and Ec70 were particularly efficient donors,
 227 representing 19% and 7.3% of total spacers, respectively (sd = 9% and 2.4%, n = 5 recordings).
 228 Based on this mapping, we could also identify which predicted plasmids were or were not being
 229 transferred. For instance, IncFII-type plasmids in Ec35, Ec75, Ec77 appear to transfer readily to
 230 EcRec, while col-type plasmids in Ec21, Ec75, and Ec77 do not appear to mobilize. Importantly,
 231 we qualitatively detect the same transfer profile for Ec70 in this community recording as in the
 232 single donor recording. However, all spacers mapping to the IncX3 plasmid in Ec70 were
 233 removed due to redundant mapping to other plasmids in the community.
 234



235
 236

237 **Figure 3: Recording of HGT events in a defined multispecies community.** Spacer recording in a
 238 defined community of 8 *E. coli* strains. Exogenous spacers (n = 14,463 pooled over 5 biological
 239 replicates) were mapped to contigs identified as plasmids²⁶ in the 8 genomes allowing only unique hits.
 240 Hits were observed for all donors except the negative control REL606, which carries no mobile genetic
 241 elements. The normalized spacer mapping is spacers per kb per 1000 exogenous spacers. Red data
 242 points denote zero recorded spacers.

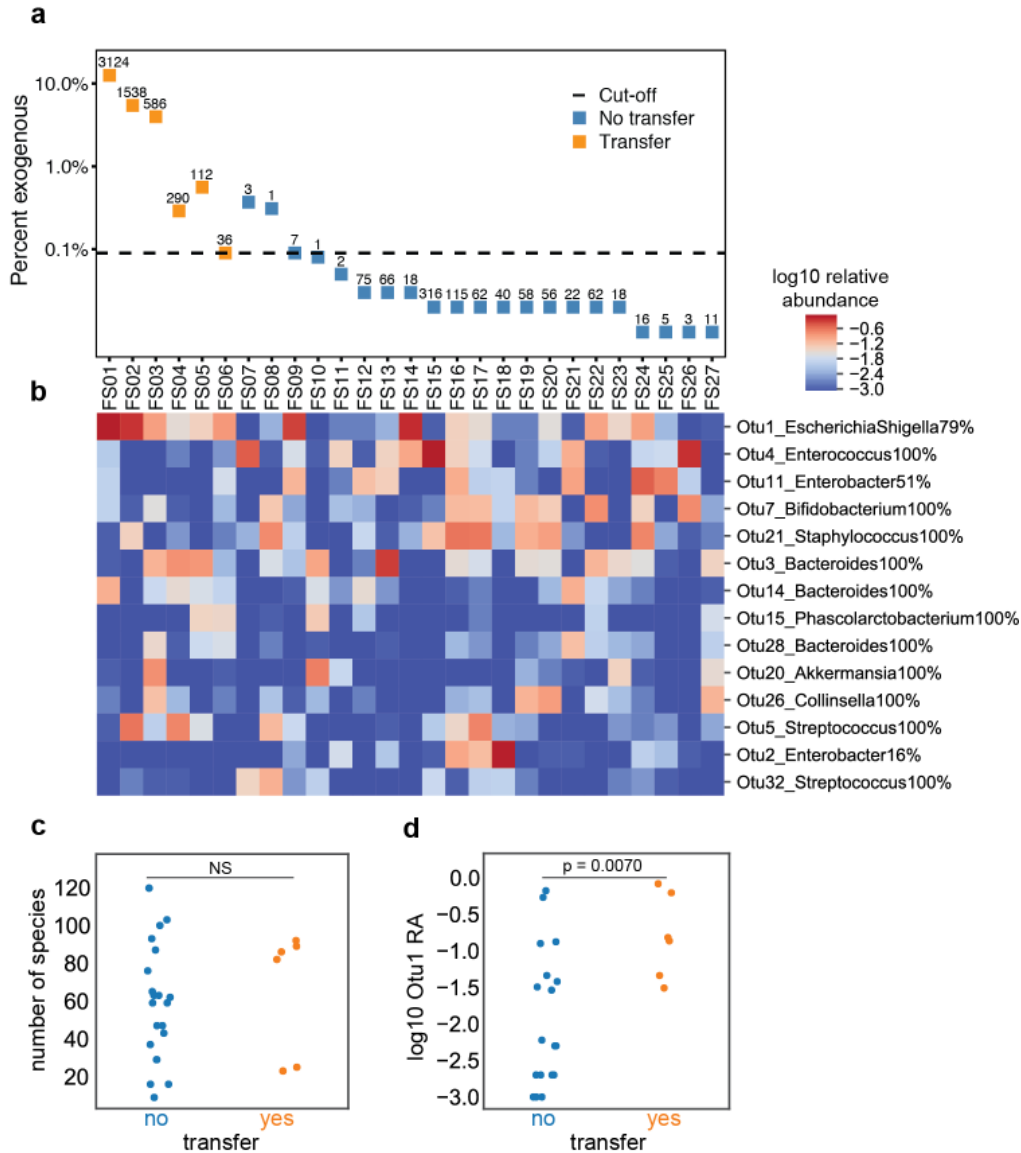
243
 244

Capturing HGT events from natural microbial communities

245 Extensive HGT has been reported in the human microbiome and has been shown to
 246 facilitate the spread of clinically important genes such as antibiotic resistance genes^{3,4,28-30}.
 247 Therefore, we sought to explore the natural mobilome of the human fecal microbiome in
 248 clinically relevant populations using the CRISPR-recording system. Fecal samples were
 249 obtained from hospitalized adults with diarrhea whose stools were tested for *Clostridium difficile*
 250 infection (CDI). Of 27 patients samples, 24 had received broad-spectrum antibiotic treatment in

251 the month prior to sampling while the remaining (FS05, FS06, and FS07) did not receive
252 antibiotics. For each sample, ~0.5 g of fecal matter was washed in PBS three times to remove
253 potential inhibiting compounds, such as antibiotics. The washed samples were each mixed with
254 the EcRec, spotted on LB agar, and incubated for 24 hours. In order to confidently identify
255 samples with HGT events we established strict criteria requiring that at least 10 exogenous
256 spacers were identified and that the percentage of exogenous spacers was at least 3 times
257 higher than in the no-donor control samples (0.03%). From the 27 recordings, we sequenced
258 >10 million CRISPR arrays (**Fig. 5a**). Six recordings pass our criterion representing a total of
259 20,991 exogenous spacers yielding 5,686 unique spacers (**Suppl. Table 2**).

260 We hypothesized that the presence of closely related donor species would be important
261 to observing HGT. We thus profiled the composition of all 27 fecal samples using 16S rRNA
262 amplicon sequencing (**Fig. 5b**). Overall, the α -diversity (number of species) was similar
263 regardless of whether high numbers of exogenous spacers were observed (**Fig. 5b, c**).
264 However, as predicted, we found that the relative abundance of the *Escherichia/Shigella* taxa
265 (Otu1) was significantly elevated in the 6 samples passing the recording criteria (**Fig. 5d**, $p =$
266 0.007, Mann–Whitney U test). Still, some samples with high abundance of *Escherichia/Shigella*
267 had few exogenous spacers (e.g. FS09 and FS14), suggesting that presence of
268 *Escherichia/Shigella* at high abundance is correlated with but not sufficient for detectable
269 transfer (e.g. presence and mobilization of plasmids may be variable in this host).



270

271 **Figure 4. Measurement of HGT events in 27 clinical fecal samples.** (a) Identifying fecal samples with
 272 robust exogenous spacer acquisition. Percent of spacers classified as exogenous for each sample.
 273 Samples with at least 0.09 % exogenous spacers and a minimum of 10 unique exogenous spacers
 274 (denoted above each data point) were classified as samples with HGT events (orange data points). (b)
 275 Cluster map of 16S OTU abundance for the 27 fecal samples. Samples with observable transfer (FS01-
 276 FS06) or no observable transfer (FS07-FS27) are shown. OTUs observed at >0.05 relative abundance in
 277 at least 2 samples are shown; log₁₀ relative abundance is displayed. (c) Number of unique operational
 278 taxonomic units (OTUs) per samples stratified on transfer status. (d) Relative abundance of Otu1
 279 (*Escherichia/Shigella*) stratified transfer status. Samples with transfer have a significant higher
 280 abundance of *Escherichia/Shigella* ($p = 0.0070$, Mann–Whitney U test).

281

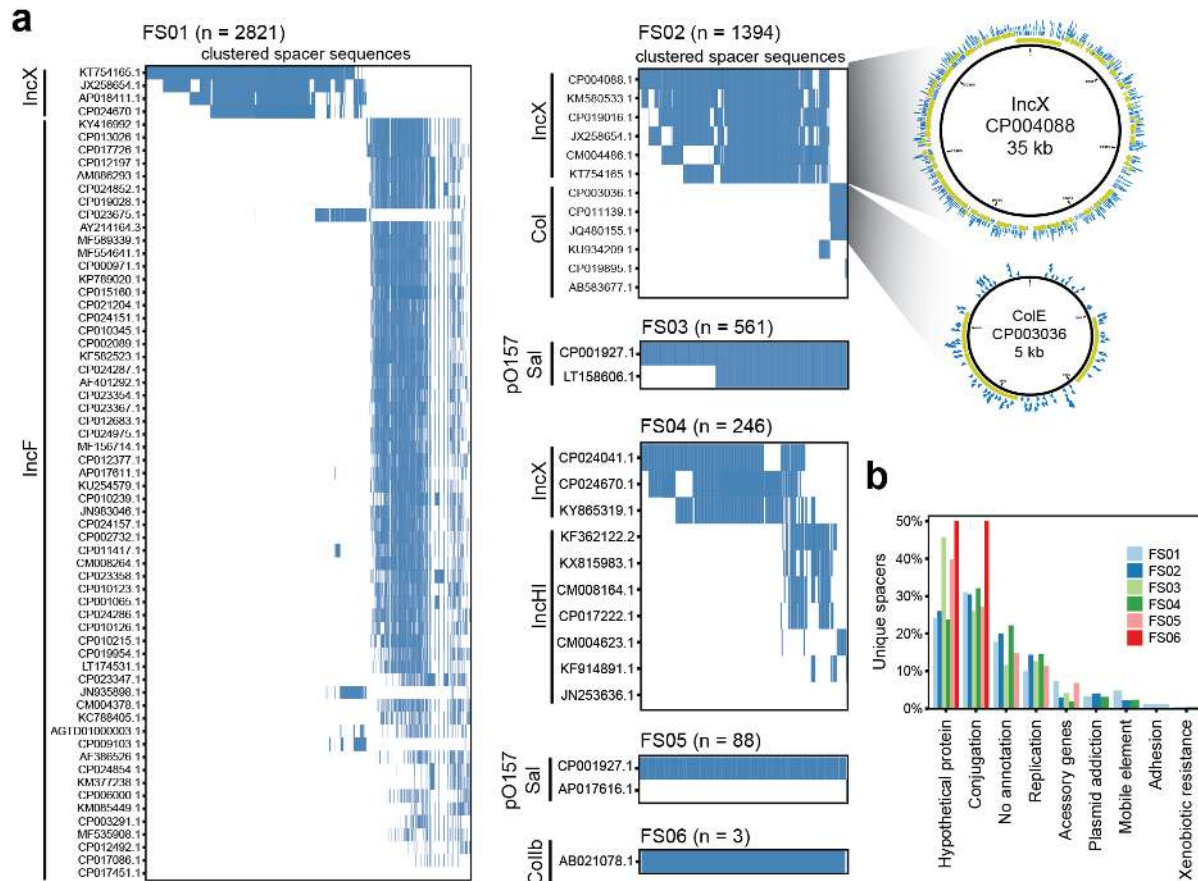
282 To identify the source of exogenous spacers, we used BLAST to search the NCBI
 283 RefSeq bacterial genome database, NCBI RefSeq viral genome database and a custom
 284 plasmid database applying the previously established thresholds (Materials and Methods).

285 Overall, the majority of the 5,686 unique exogenous spacers could be matched to at least one of
286 the databases (**Suppl. Table 2**). All spacers with hits to the viral database also matched to the
287 genome database. Furthermore, >95% of spacers with hits to the genome database also
288 matched to the plasmid database, highlighting that the identifiable spacers were most likely of
289 plasmid origin. For each sample, we identified the minimal set of reference plasmids that
290 encompass all spacers. Clustered heatmaps from these plasmid hits were used to identify the
291 likely source of the exogenous spacers and predict the number of discrete mobile genetic
292 elements. For each sample, we infer that 1-2 different plasmids were transferred (**Fig. 5a**).

293 For instance, BLAST hits of spacers to the plasmid database in sample FS02 indicate
294 that two plasmids were transferred, a large IncX-type plasmid and a small colE-type plasmid
295 (**Fig. 5a**). The putative IncX hits match to a 35 kb plasmid (Genbank accession CP004088)
296 carrying no resistance markers. The acquired spacers almost completely tile the plasmid back-
297 bone, suggesting that the reference is a good representation of the transferred plasmid. The
298 small colE-like plasmid (Genbank accession CP003036) has three predicted open reading
299 frames (ORFs): a replication protein, a mobilization protein and an unknown ORF. While spacer
300 coverage of the colE plasmid is sparser than the IncX plasmid, spacers matched across the
301 back-bone suggesting that all regions of the pCE10B plasmid were present in the mobilized
302 plasmid captured from FS02. Interestingly, the smaller plasmid does not encode a conjugation
303 apparatus and therefore requires conjugation genes *in trans* for mobilization. Mapping all
304 acquired spacers to the Plasmid Finder database²⁶ revealed matches to IncX, IncI, IncF, IncH,
305 pO157_Sal, and colE plasmid types, which are all common replicons in *Enterobacteriaceae*
306 (**Fig. 5a**).

307 To better delineate the functions of the ORFs that yielded spacers, we used the RefSeq
308 database to extract the functional annotations of genes with spacer hits (**Fig. 5b** and **Suppl.**
309 **Table 4**). For each sample, 80-85% of spacers had functional annotations. The most common
310 gene annotations were canonically associated with plasmids including conjugation, replication
311 and plasmid addiction genes. As expected, a large portion of the ORFs had no known function
312 (**Fig. 5b**). Given that the majority of patients received antibiotics recently (4/6 with detectable
313 transfer), one might expect that these samples would be enriched in HGT for antibiotic
314 resistance genes. Interestingly, mapping spacers against the ResFinder database³¹ yielded only
315 two spacer hits to antibiotic resistance genes, a bla_{TEM} beta-lactamase and a chloramphenicol
316 acetyltransferase gene (both from FS04), suggesting that, although present, resistance genes
317 are not particularly enriched in these HGT pools.

318



319

320

321 **Figure 5. Analysis of human-associated mobilome from HGT recordings.** (a) Exogenous spacers
 322 mapped to the custom plasmid database, each row represents a plasmid (denoted by accession number).
 323 The mappings are filtered to include the fewest number of plasmids covering all spacers. Rows are sorted
 324 in order of the number of spacers that map to the plasmid. The sorting enables easy identification of
 325 discrete transferred elements. Each spacer cluster is annotated with the predicted plasmid group based
 326 on Plasmid Finder²⁶. Spacer mapping is illustrated for FS02 showing the plasmid backbone with predicted
 327 ORFs (yellow) and mapping spacers (blue). (b) Annotation categories overlapping with the spacers from
 328 all six clinical recordings. Genes predicted to be involved in conjugative transfer dominate, followed by
 329 unannotated genes and genes involved in plasmid replication. Notably, very few spacers overlap with
 330 genes involved in drug resistance.

331

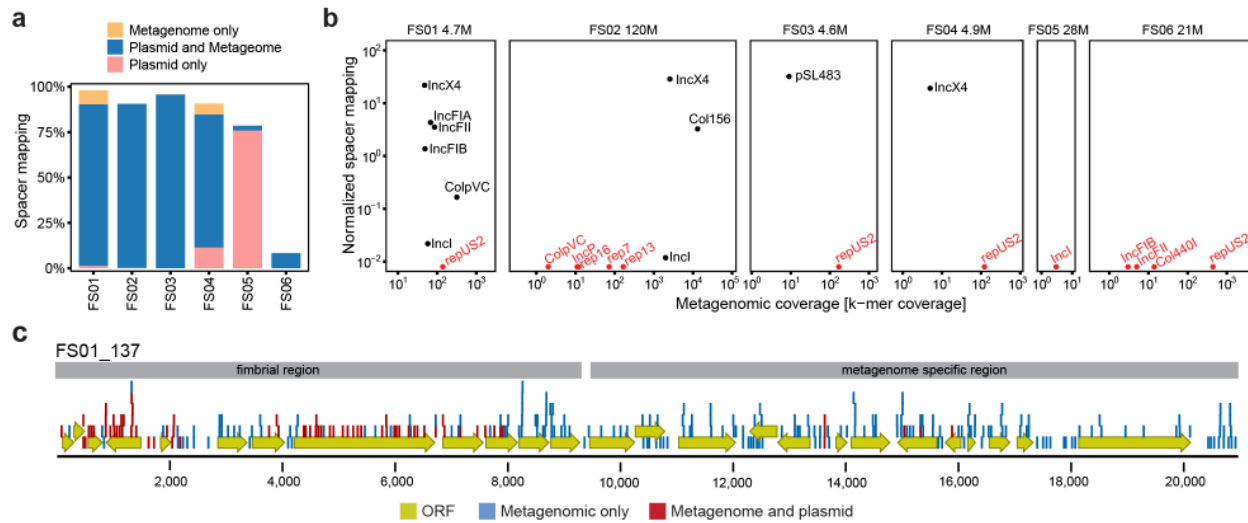
332 Systematic identification of transferred plasmids from metagenomes

333 We further performed shotgun metagenomic sequencing on the original fecal samples to assess
 334 the recovery of spacers against assembled contigs and to confirm the presence of putative
 335 plasmids in the samples. Metagenomic reads were assembled yielding ~371 Mbps of contigs
 336 across the six samples with recordable HGT events (FS01-FS06) (**Suppl. table 8**). Most
 337 acquired spacers could be matched to metagenomic contigs by BLAST (**Fig. 6a**). However, in
 338 two samples, FS05 and FS06, the metagenomic recovery rate was very low (3% and 8%,
 339 respectively). Correspondingly, these samples also had few acquired unique exogenous

340 spacers (112 and 36, respectively), suggesting low frequency of HGT. Mapping of all
341 exogenous spacers to the plasmid database revealed that the majority of spaces matched to
342 both metagenomic contigs and published plasmids, confirming that most HGT was via plasmids
343 (**Fig. 6a**).

344 Using the Plasmid Finder database²⁶, we identified putative plasmid contigs across the
345 metagenomes. We observed transfer of a variety of Enterobacteriaceae plasmids including
346 IncF, IncX, IncI, and col types, corroborating the results generated from using our custom
347 plasmid database (**Fig. 6b**). In addition, we also detected a number of non-transferred plasmids
348 (e.g. repUS2) from Gram-positive species including *S. aureus*. Interestingly, certain plasmid
349 types appeared to transfer more readily than others based on comparing their spacer mapping
350 density and metagenomic coverage. In particular, IncX-type plasmids transferred efficiently
351 since we observed nearly the same spacer density across three orders of magnitude in
352 metagenomic coverage (**Fig. 6b**, FS01, FS02 and FS04). In contrast, IncI-type plasmids
353 transferred at very low levels despite the metagenomic coverage varying two orders of
354 magnitude between FS01 and FS02 (**Fig. 6b**).

355 A number of spacers mapped only to the metagenomic contigs (and not to the plasmid
356 database; **Fig. 6a** and **Suppl. fig S5**). Among those contigs, one contig from FS01 had a
357 majority of metagenomic-only spacers (202/276) indicating that the contig was not normally
358 found on plasmids (**Fig. 6c**). This contig consists of a region encoding a P-type fimbria along
359 with a transposase as well as a region containing mostly hypothetical proteins. The former
360 region has been found in other plasmids, as indicated by spacer mapping to the plasmid
361 database, while the latter region appears to be specific to the FS01 sample (**Fig. 6c**). The contig
362 is not classified as plasmid, however, it is likely an incomplete assembly of a larger plasmid.
363 This highlights the utility of our approach to identify novel transferred elements that may not be
364 predicted by traditional reference-based methodologies.



365

366 **Figure 6. Metagenomic verification of predicted transfer events.** (a) Percentage of spacers that could
 367 be mapped to the metagenomic contigs only (yellow), plasmid database and metagenomic contigs (blue),
 368 or plasmid database only (pink). (b) Mapping of spacers to predicted metagenomic plasmid contigs as a
 369 function of contig coverage in the assembly. The normalized spacer mapping is spacers per kb per 1000
 370 exogenous spacers. Red data points denote zero recorded spacers. Number above each plot denotes the
 371 number of reads in the metagenome (millions). (c) Contig from FS01 where the majority of spacers were
 372 specific to the metagenome (blue). The contig consists of a region encoding a P-type fimbria and a region
 373 containing most hypothetical proteins specific to the metagenome.

374

375 Estimating transfer frequencies in complex microbiomes

376 To assess the overall rate of HGT, including transient transfers, in our human fecal
 377 samples, we sequenced spacers from each fecal recording without gel extraction of the
 378 expanded arrays to calculate a rate of spacer acquisition (**Suppl. table 6**). The array expansion
 379 frequency ($[\# \text{ of expanded arrays}] / [\text{total } \# \text{ of arrays}]$) is multiplied by the frequency of unique
 380 exogenous spacers ($[\# \text{ of unique exo. spacers}] / [\# \text{ of expanded arrays}]$) to estimate the
 381 proportion of recording cells that captured exogenous spacers. For the six samples with high
 382 frequencies of exogenous spacers (FS01-FS06), the population-estimates of HGT spanned
 383 4×10^{-6} to 10^{-3} $[\text{unique exo. spacers}] / [\text{total } \# \text{ of arrays}]$ (**Suppl. table 7**). Together, these results
 384 suggest that while HGT may only be detected in some communities (e.g. 6 of 27 communities in
 385 this study), the extent of transfer in HGT-active communities can be quite high.

386

387 Discussion

388 While comparative analyses of sequenced genomes have provided strong evidence of
 389 the abundant HGT^{3,4}, the true rates of horizontal transfer of mobile DNA in a given community is
 390 poorly understood since many events may not fix in the population and diverse mobile elements
 391 compete for persistence in recipients. Our CRISPR-based recording system captures HGT

392 events stably into genomic arrays that can be used to assess transfer rates and identity of
393 mobile elements, far beyond current methodologies that rely on phenotypic selection of markers
394 (e.g. co-transfer of antibiotic resistance genes). The ability to detect, in real-time, transient
395 transfer events and those occurring at low frequencies enables an in-depth characterization of
396 HGT in complex microbiomes. In this study, we showed that HGT can be resolved down to
397 individual mobile plasmids from donors that can carry up to 6 putatively mobile plasmids. We
398 find that the different microbial donors varied in transfer efficiencies of different plasmids, which
399 might reflect differences in HGT efficiency between donor plasmids and/or competition for
400 recipients. Such an approach could more generally facilitate detailed mechanistic studies of
401 spread of mobile DNA associated with virulence phenotypes in specific pathogens.

402 When our approach is applied to clinical fecal specimens, we were able to identify active
403 HGT in 22% of the samples (6 out of 27). In many instances, we observed multiple discrete
404 plasmids being transferred, most of which interestingly did not carry selectable markers such as
405 antibiotic resistance genes. This is surprising given the extensive usage of antibiotics in the
406 cohort (24/27 patients). This finding suggests that a substantially larger pool of active and
407 mobile plasmids exist in the gut microbiome beyond just the antibiotic resistance plasmids that
408 are typically identified by phenotypic assays in experimental studies of HGT in the gut. By
409 analyzing the captured spacers, we also find that many horizontally acquired genes have no
410 known function, in agreement with previous bioinformatic analyses³. Using metagenomic
411 sequencing, we definitively matched acquired spacer sequences to assembled plasmid contigs
412 and plasmid types involved in these HGT events. While many different plasmids were identified
413 in the metagenome, only subsets were shown to mobilize at varying efficiencies, with the IncX
414 type transferring most efficiently.

415 The sensitivity of the spacer acquisition system allowed us to estimate the frequency of
416 HGT in the human fecal samples. Because our estimates are based on adding a recipient strain
417 to the fecal community, the transfer rates might not reflect actual transfer between community
418 members, however, it does give an indication of the HGT potential of the community. We
419 estimate transfer frequencies into the recording strain between 10^{-6} - 10^{-3} unique transferred
420 spacers per recipient cell, suggesting that HGT is frequent.

421 Even though the observed mobile elements were classified plasmids, we still expect that
422 phages are an important contributor to HGT. However, there are several possible explanations
423 to why we do not observe phage-driven HGT. First, infection with phages could lead to cell lysis
424 and consequently loss of recording cells from the population. Second, given that the *E. coli*
425 CRISPR system is specific to capturing dsDNA, non-dsDNA phages (i.e. ssRNA or ssDNA

426 phages) will not be captured. Third, the washing of the fecal sample (i.e. to remove antibiotics or
427 other factors that might inhibit the recording strain) might result in the loss of most phage
428 particles. We assessed the abundance of DNA phages relative to plasmids in the clinical fecal
429 samples and found that on average there were 8 times more reads mapping to plasmids than to
430 phages, suggesting that plasmids are more abundant in the fecal samples (**Supp. fig. S6**).

431 Future improvements to the technique could improve the scope of recording. Diverse
432 CRISPR acquisition systems could be utilized to capture other HGT moieties (i.e. RNA with RT-
433 Cas systems) beyond dsDNA captured by the *E. coli* system. Additionally, endogenous or
434 engineered Cas1/Cas2 recording systems could be implemented in the context of different
435 hosts to understand the host specificity of transfer for diverse bacterial species. These various
436 systems and hosts could be multiplexed for high-resolution recording of HGT in various
437 environments, from the human gut to various environmental microbiota. CRISPR spacer
438 acquisition enables real-time recording of previously difficult to record transient HGT events,
439 and offers a powerful new approach to studying flow and transfer of complex mobilomes at an
440 unprecedented resolution.

441

442 **Acknowledgements**

443 We thank members of the Wang lab for helpful scientific discussions and feedback.
444 H.H.W. acknowledges specific funding from ONR (N00014-17-1-2353), NSF (MCB-1453219),
445 and NIH (1R01AI132403-01). C.M. acknowledges funding from the Carlsberg Foundation.
446 R.U.S. is supported by a Fannie and John Hertz Foundation Fellowship and a NSF Graduate
447 Research Fellowship (DGE-1644869). C.M. thanks Dr. Kristian Schønning, Hvidovre Hospital,
448 Denmark, for gifting the clinical *E. coli* strains.

449

450 **Author contributions**

451 C.M, R.U.S., and H.H.W. developed the initial concept. D.F. provided clinical samples
452 and associated antibiotic treatment data. C.M, and R.U.S. performed experiments and analyzed
453 the results under the supervision of H.H.W.; C.M., R.U.S. and H.H.W. wrote the manuscript with
454 input from all authors.

455

456 **Competing financial interests:**

457 The authors declare no competing financial interests.

458 References

- 459 1. Shoemaker, N. B., Vlamakis, H., Hayes, K. & Salyers, A. A. Evidence for extensive
460 resistance gene transfer among *Bacteroides* spp. and among *Bacteroides* and other
461 genera in the human colon. *Applied and Environmental Microbiology* **67**, 561–568 (2001).
- 462 2. Coyne, M. J., Zitomersky, N. L., McGuire, A. M., Earl, A. M. & Comstock, L. E. Evidence
463 of extensive DNA transfer between bacteroidales species within the human gut. *mBio* **5**,
464 e01305–14 (2014).
- 465 3. Brito, I. L. *et al.* Mobile genes in the human microbiome are structured from global to
466 individual scales. *Nature* **535**, 435–439 (2016).
- 467 4. Smillie, C. S. *et al.* Ecology drives a global network of gene exchange connecting the
468 human microbiome. *Nature* **480**, 241–244 (2011).
- 469 5. Thomas, C. M. & Nielsen, K. M. Mechanisms of, and Barriers to, Horizontal Gene
470 Transfer between Bacteria. *Nature Reviews Microbiology* **3**, 711–721 (2005).
- 471 6. Hehemann, J.-H. *et al.* Transfer of carbohydrate-active enzymes from marine bacteria to
472 Japanese gut microbiota. *Nature* **464**, 908–912 (2010).
- 473 7. Schmidt, H. & Hensel, M. Pathogenicity islands in bacterial pathogenesis. *Clinical*
474 *Microbiology Reviews* **17**, 14–56 (2004).
- 475 8. Wellington, E. M. H. *et al.* The role of the natural environment in the emergence of
476 antibiotic resistance in gram-negative bacteria. *The Lancet Infectious Diseases* **13**, 155–
477 165 (2013).
- 478 9. Martinez, R. J. *et al.* Horizontal gene transfer of PIB-type ATPases among bacteria
479 isolated from radionuclide- and metal-contaminated subsurface soils. *Applied and*
480 *Environmental Microbiology* **72**, 3111–3118 (2006).
- 481 10. Tettelin, H. *et al.* Genome analysis of multiple pathogenic isolates of *Streptococcus*
482 *agalactiae*: implications for the microbial "pan-genome". *Proceedings of the National*
483 *Academy of Sciences* **102**, 13950–13955 (2005).
- 484 11. Rasko, D. A. *et al.* The pangenome structure of *Escherichia coli*: comparative genomic
485 analysis of *E. coli* commensal and pathogenic isolates. *Journal of Bacteriology* **190**,
486 6881–6893 (2008).
- 487 12. Lapierre, P. & Gogarten, J. P. Estimating the size of the bacterial pan-genome. *Trends*
488 *Genet.* **25**, 107–110 (2009).
- 489 13. Nielsen, K. M. & Townsend, J. P. Monitoring and modeling horizontal gene transfer.
490 *Nature Biotechnology* **22**, 1110–1114 (2004).
- 491 14. Ravenhall, M., Škunca, N., Lassalle, F. & Dessimoz, C. Inferring horizontal gene transfer.
492 *PLoS Comput Biol* **11**, e1004095 (2015).
- 493 15. Koonin, E. V., Makarova, K. S. & Wolf, Y. I. Evolutionary Genomics of Defense Systems
494 in Archaea and Bacteria. *Annu. Rev. Microbiol.* **71**, 233–261 (2017).
- 495 16. Marraffini, L. A. & Sontheimer, E. J. CRISPR interference limits horizontal gene transfer
496 in staphylococci by targeting DNA. *Science* **322**, 1843–1845 (2008).
- 497 17. Touchon, M. *et al.* CRISPR distribution within the *Escherichia coli* species is not
498 suggestive of immunity-associated diversifying selection. *Journal of Bacteriology* **193**,
499 2460–2467 (2011).
- 500 18. Yosef, I., Goren, M. G. & Qimron, U. Proteins and DNA elements essential for the
501 CRISPR adaptation process in *Escherichia coli*. *Nucleic Acids Research* **40**, 5569–5576
502 (2012).
- 503 19. Sheth, R. U., Yim, S. S., Wu, F. L. & Wang, H. H. Multiplex recording of cellular events
504 over time on CRISPR biological tape. *Science* **358**, 1457–1461 (2017).
- 505 20. Brouns, S. J. J. *et al.* Small CRISPR RNAs guide antiviral defense in prokaryotes.
506 *Science* **321**, 960–964 (2008).
- 507 21. Levy, A. *et al.* CRISPR adaptation biases explain preference for acquisition of foreign

- 508 DNA. *Nature* **520**, 505–510 (2015).
- 509 22. Datta, N., Hedges, R. W., Shaw, E. J., Sykes, R. B. & Richmond, M. H. Properties of an
510 R Factor from *Pseudomonas aeruginosa*. *Journal of Bacteriology* **108**, 1244–1249
511 (1971).
- 512 23. Herrero, M., de Lorenzo, V. & Timmis, K. N. Transposon vectors containing non-antibiotic
513 resistance selection markers for cloning and stable chromosomal insertion of foreign
514 genes in gram-negative bacteria. *Journal of Bacteriology* **172**, 6557–6567 (1990).
- 515 24. Simon, R., Priefer, U. & Pühler, A. A Broad Host Range Mobilization System for In Vivo
516 Genetic Engineering: Transposon Mutagenesis in Gram Negative Bacteria. *Nat*
517 *Biotechnol* **1**, 784–791 (1983).
- 518 25. Ferrières, L. *et al.* Silent mischief: bacteriophage Mu insertions contaminate products of
519 *Escherichia coli* random mutagenesis performed using suicidal transposon delivery
520 plasmids mobilized by broad-host-range RP4 conjugative machinery. *Journal of*
521 *Bacteriology* **192**, 6418–6427 (2010).
- 522 26. Carattoli, A. *et al.* In silico detection and typing of plasmids using PlasmidFinder and
523 plasmid multilocus sequence typing. *Antimicrob. Agents Chemother.* **58**, 3895–3903
524 (2014).
- 525 27. Bradley, D. E., Taylor, D. E. & Cohen, D. R. Specification of surface mating systems
526 among conjugative drug resistance plasmids in *Escherichia coli* K-12. *J. Bacteriol.* **143**,
527 1466 (1980).
- 528 28. Lester, C. H., Frimodt-Møller, N., Sørensen, T. L., Monnet, D. L. & Hammerum, A. M. In
529 vivo transfer of the *vanA* resistance gene from an *Enterococcus faecium* isolate of animal
530 origin to an *E. faecium* isolate of human origin in the intestines of human volunteers.
531 *Antimicrob. Agents Chemother.* **50**, 596–599 (2006).
- 532 29. Gumpert, H. *et al.* Transfer and Persistence of a Multi-Drug Resistance Plasmid in situ of
533 the Infant Gut Microbiota in the Absence of Antibiotic Treatment. *Front. Microbio.* **8**, 1852
534 (2017).
- 535 30. Porse, A. *et al.* Genome Dynamics of *Escherichia coli* during Antibiotic Treatment:
536 Transfer, Loss, and Persistence of Genetic Elements In situ of the Infant Gut. *Front. Cell.*
537 *Infect. Microbiol.* **7**, 599 (2017).
- 538 31. Zankari, E. *et al.* Identification of acquired antimicrobial resistance genes. *J. Antimicrob.*
539 *Chemother.* **67**, 2640–2644 (2012).
- 540 32. Edgar, R. C. Search and clustering orders of magnitude faster than BLAST.
541 *Bioinformatics* **26**, 2460–2461 (2010).
- 542 33. R Core Team. R: A Language and Environment for Statistical Computing.
- 543 34. Wickham, H. *ggplot2: Elegant Graphics for Data Analysis*. (Springer New York, 2009).
544 doi:10.1007/978-0-387-98141-3
- 545 35. Ji, B. W., Sheth, R. U., Dixit, P. D., Wang, H. H. & Vitkup, D. Quantifying spatiotemporal
546 dynamics and noise in absolute microbiota abundances using replicate sampling. (2018).
547 doi:10.1101/310649
- 548 36. Kozich, J. J., Westcott, S. L., Baxter, N. T., Highlander, S. K. & Schloss, P. D.
549 Development of a dual-index sequencing strategy and curation pipeline for analyzing
550 amplicon sequence data on the MiSeq Illumina sequencing platform. *Applied and*
551 *Environmental Microbiology* **79**, 5112–5120 (2013).
- 552 37. Wang, Q., Garrity, G. M., Tiedje, J. M. & Cole, J. R. Naive Bayesian Classifier for Rapid
553 Assignment of rRNA Sequences into the New Bacterial Taxonomy. *Applied and*
554 *Environmental Microbiology* **73**, 5261–5267 (2007).
- 555 38. Baym, M. *et al.* Inexpensive Multiplexed Library Preparation for Megabase-Sized
556 Genomes. *bioRxiv* 013771 (2015). doi:10.1101/013771
- 557 39. Bolger, A. M., Lohse, M. & Usadel, B. Trimmomatic: a flexible trimmer for Illumina
558 sequence data. *Bioinformatics* **30**, 2114–2120 (2014).

- 559 40. Bankevich, A. *et al.* SPAdes: a new genome assembly algorithm and its applications to
560 single-cell sequencing. *J. Comput. Biol.* **19**, 455–477 (2012).
- 561 41. Li, H. Aligning sequence reads, clone sequences and assembly contigs with BWA-MEM.
562 *preprint arXiv*. (2013).
- 563 42. Wick, R. R., Judd, L. M., Gorrie, C. L. & Holt, K. E. Unicycler: Resolving bacterial genome
564 assemblies from short and long sequencing reads. *PLoS Comput Biol* **13**, e1005595
565 (2017).
- 566
- 567

568 **Materials and methods**

569 **Strains**

570 The recording strain (EcRec) was BL21 (NEB C2530H) with the pRec Δ lacl plasmid
571 (Addgene #104575)¹⁹. Clinical *E. coli* isolates were a kind gift from Dr. Kristian Schønning,
572 Hvidovre Hospital, Denmark. See **Suppl. table 5** for full overview of donor strains.

573

574 **Defined recordings**

575 All strains were grown in LB medium with appropriate antibiotics and washed in PBS
576 prior to recording. In all recordings an overnight culture of the recording strain was diluted 1:50
577 and grown for one hour, then anhydrotetracycline (aTc) was added to a final concentration of
578 100 ng / mL and the strain was incubated for another hour. Next, the recording strain and donor
579 strain were mixed 1:1 at OD600 = 0.5, except in the ratio experiment (**Suppl. Fig. S1**) where
580 strains were mixed in the ratios described in the figure. After mixing, the mixture was spotted on
581 LB agar + 100 ng / mL aTc. Plates were incubated for 6 h at 37 C. At the end of a recording, the
582 cells were scraped off the plate and resuspended in 100 μ l PBS and heat inactivated at 95 C.
583 for 3 min, subsequently they were stored at -20 C until sequencing analysis.

584

585 **Fecal recordings**

586 The donor strain was prepared as described above. All fecal recordings were performed
587 within 24 h of collecting the fecal samples. For each sample ~0.5 g were washed 2 times in 1 ml
588 PBS and finally resuspended in 100 μ l LB + 100 ng / ml aTc. The washed fecal sample was
589 mixed with a 100 μ l resuspension of 1 mL OD600 = 0.5 of the recording strain. From this
590 mixture 50 μ l was plated on LB agar + 100 ng / mL aTc and incubated for 24 h at 37 C.
591 Subsequently, the samples were processed as described above.

592

593 **Ethical Review**

594 The protocol for the collection of human samples and data was approved by the
595 Columbia Institutional Review Board with a waiver of informed consent (IRB
596 AAAR9489). Residual (waste) fecal specimens were used following standard clinical testing,
597 and anonymized data was retrieved retrospectively.

598

599 **Array sequencing**

600 CRISPR arrays were sequenced utilizing our established sequencing pipeline¹⁹ with
601 minor modification. Briefly, DNA from cells was obtained by enzymatic and heat lysis, barcoded

602 PCR amplification of CRISPR arrays was performed, samples were pooled and sequencing was
603 performed on the Illumina MiSeq platform (MiSeq v2 50 cycle, MiSeq v2 300 cycle or MiSeq v3
604 150 cycle kits) with additional spike-in of custom sequencing primers. In addition, to enrich for
605 expanded spacers, double gel extraction of expanded spacer bands on an E-gel EX Agarose
606 Gel 2% was performed on pooled libraries. An overview of sequencing runs and sample
607 statistics can be found in **Suppl. tables 1, 2, 6**

608

609 **Data processing**

610 Spacers were extracted utilizing our established spacer extraction pipeline; code can be
611 accessed at <https://github.com/ravisheth/trace>. Extracted spacers were filtered against the
612 genome of the recording strain (quality filtered reads from sequencing of the same EcRec
613 BL21/pRecΔlacI) using a two-step process using USEARCH v10.0.240³². First spacers were
614 filtered using a database of word size 8, then all non-hit spacers were collected and filtered
615 against the same database using word size 5 (e.g. 'usearch -usearch_global -id 0.8 -query_cov
616 0.8 -top_hit_only -maxrejects 0 -strand both -uc out.uc'). Subsequently the identified exogenous
617 spacers were uniqued e.g.('usearch -fastx_uniques -fastaout centroids.fa -sizeout'). The unique
618 exogenous spacers was utilized in all subsequent spacer mapping performed with BLAST
619 2.7.1+ ('blastn -db -query -perc_identity 90 -max_target_seqs 500000000 -task blastn -
620 word_size 10 -outfmt "6 std sstrand qlen slen"). The output of BLAST was filtered to ensure 95
621 % identity and 95 % coverage of the query spacer. An example of the processing workflow can
622 be seen in **Suppl. Fig S1**. Data analysis was performed in R³³ using ggplot2³⁴ and CLC main
623 workbench (www.qiagenbioinformatics.com).

624

625 **Reference databases**

626 The following reference databases were used to identify the source of the acquired
627 spacers: Prokaryotic RefSeq Genomes from January 2018;
628 <ftp://ftp.ncbi.nlm.nih.gov/genomes/refseq/bacterial/>. Viral RefSeq Genomes from January 2018;
629 <ftp://ftp.ncbi.nlm.nih.gov/genomes/refseq/viral/>. A custom plasmid database was created using
630 the following search criteria in NCBI GenBank nucleotide database from January 2018;
631 'plasmid[TI]', then summary file was downloaded and parsed to get accession numbers of all
632 circular elements:
633 'grep -A1 'bp circular DNA' summary.txt | grep -v 'bp circular DNA' | grep -v '\\-' | cut -d ' ' -f1 >
634 output.txt' which were subsequently retrieved with NCBI batch
635 (<https://www.ncbi.nlm.nih.gov/sites/batchentrez>).

636

637 **16S rRNA sequencing**

638 16S rRNA sequencing was performed utilizing our established sequencing pipeline;
639 detailed methods can be found in our previous publication³⁵. Briefly, genomic DNA (gDNA) was
640 extracted with a protocol utilizing the Qiagen MagAttract PowerMicrobiome DNA/RNA kit
641 (Qiagen 27500-4-EP). Samples were bead beat with 0.1mm Zirconia Silica Beads (Biospec
642 11079101Z) for a total of ten minutes (Biospec 1001); the Qiagen kit protocol was followed but
643 at reduced volumes on a Biomek 4000 liquid handling robot. The resulting gDNA was subjected
644 to 16S V4 amplicon sequencing utilizing custom barcoded primers³⁶ and NEBNext Q5 Hot Start
645 HiFi Master Mix (NEB M0543L). Resulting PCR products were quantified and pooled on a
646 Biomek 4000 robot and sequenced utilizing an Illumina MiSeq V2 300 cycle kit. The sequencing
647 data was analyzed using USEARCH 10.0.240³²; reads were merged (-fastq_mergepairs),
648 filtered (-fastq_filter -fastq_maxee 1.0 -fastq_minlen 240), and 100% ZOTUs were generated (-
649 unoise3) and OTU table created (-otutab). Taxonomy was assigned to ZOTUs using the RDP
650 classifier³⁷. The OTU table was rarefied to 1000 reads per sample before analysis.

651

652 **Whole genome and shotgun metagenomic sequencing**

653 The recording strain BL21/pRec along with all donor strains were subjected to whole
654 genome sequencing (**Suppl. table 5**) and clinical samples were subjected to shotgun
655 metagenomic sequencing (**Suppl. table 8**). gDNA was extracted from individual isolates or fecal
656 samples utilizing the gDNA extraction pipeline detailed above. Sequencing preparation followed
657 a published protocol for low-volume Nextera library preparation³⁸. Barcoded samples were
658 pooled and sequencing was performed on the Illumina MiSeq (2x150 reads), Illumina NextSeq
659 (2x75 reads) or Illumina HiSeq X platform (2x150 reads). Adapters were trimmed utilizing
660 Trimmomatic³⁹. Draft assemblies for the donor strains were conducted using SPAdes utilizing
661 the --careful flag⁴⁰. Metagenomes were assembled with SPAdes utilizing the --meta flag. Raw
662 metagenomic reads were mapped to the refseq viral database as well as the plasmid database
663 using bwa mem⁴¹.

664 The donor strain Ec70 was further sequenced utilizing the Oxford MinION platform;
665 genomic DNA was extracted with a Gentra Puregene kit (Qiagen), prepared for sequencing
666 utilizing the RAD004 kit and sequenced on a single R9.4.1 flow cell. For this strain, hybrid
667 assembly of the genome and individual plasmids was conducted utilizing UniCycler⁴². See
668 **Suppl. table 5** for genome sequencing information and **Suppl. table 8** for metagenome
669 sequencing information.

670 **Data availability**

671 Assembled genomes, metagenomic reads, and CRISPR array sequencing will be made
672 available at the time of publication through NCBI SRA.